RADAR-BRIGHT AND RADAR-DARK HALOES AROUND CRATERS ON LUNAR NEARSIDE: IMPLICATIONS ON PARTICLE-SIZE DISTRIBUTION OF EJECTA.
V. Gupta[1] and R. R. Ghent[1], [1]Univeristy of Toronto, Department of Geology, 22 Russell Street, Toronto, ON, Canada, M5S 3B1, gupta@geology.utoronto.ca, ghentr@geology.utoronto.ca.

Introduction: Distinct radar-bright [1, 2] and radar-dark ejecta facies [3] have been observed to form haloes around numerous craters on the lunar nearside during Earth-based radar investigations. These observations provide an opportunity to quantify the block distribution in crater ejecta in order to further understand the physics of ejecta production and ballistic emplacement on an airless body. In this study, we make detailed measurements of the sizes of radar-bright and radar-dark ejecta haloes associated with a large number of craters on the lunar nearside, using newly-released Earth-based 70-cm wavelength radar imagery obtained from the Planetary Data System (PDS) archive. The ultimate goal of the study is to understand the particle size distribution in lunar ejecta blankets. This would be a stepping stone for the eventual formulation of models that depict how impact ejecta are produced and emplaced on the Moon.

Background: It is important to have a detailed understanding of particle size distribution in lunar ejecta blankets, since it can provide us with information about how particles of various sizes are produced in lunar impacts and eventually emplaced on the surface. Earth-based radar has been used in this study since the strength of the radar returns depends on the degree of scattering by particles on and near the surface. The strong dependence of these radar returns on polarization and wavelength allows for a degree of constraint through a comparison of multiple polarizations and wavelengths. Bright signatures are produced by particles on or near the surface large enough to scatter the radar [e.g. 2], whereas dark responses appear due to a lack of these big blocks [3]. We predict that the percentage of coarse material decreases with distance away from the crater, leaving only the fine-grained material to travel the farthest. The edge of either halo is the point at which we begin to see either an abundance of blocks (bright haloes) or a lack of blocks (dark haloes), and the transition between the two can be either sharp or gradational, thereby indicating two potentially different types of processes involving ejecta production and emplacement.

Previous work [3-5] showed that nearly all lunar impacts over two orders of magnitude in size produce block-poor, radar-dark ejecta haloes that had not been previously studied. Is has been demonsrated [4, 5] that for a small number of large craters, the total volume of block-poor ejecta scales with crater size according to the power-law relationship:

$$r_H = Ar_c^{1.25} \qquad (1)$$

where $A = (k/t_H)^{1/3}$ (empirically derived), r_H is the halo radius, t_H is the ejecta thickness at the halo margins and r_c is the crater radius (from [6]). Those studies, however, did not provide any insight into how the fine material is produced. For instance, is it material that is broken up by interactions within the ejecta curtain, or is it material that is broken up upon interaction with material on the ground? Through the results obtained from this study, we aim to shed light on this question, and also to more fully understand the process of ejecta emplacement.

Method: Our work involves more detailed measurements of the sizes of a large number of radar-dark haloes associated with craters 5 km and larger in diameter, in order to determine whether or not the same scaling applies over the entire range of crater sizes. Furthermore, we investigate radar-bright haloes and determine whether or not we can apply a similar relationship between bright-halo and crater size, as with the radar-dark haloes. In addition, we make observations of the morphologies of the bright and dark haloes and the relationships between them, such as the nature of the transition from one to another. Fig. 1 is a radar image of Copernicus. The bright and dark haloes can be seen around the crater rim.

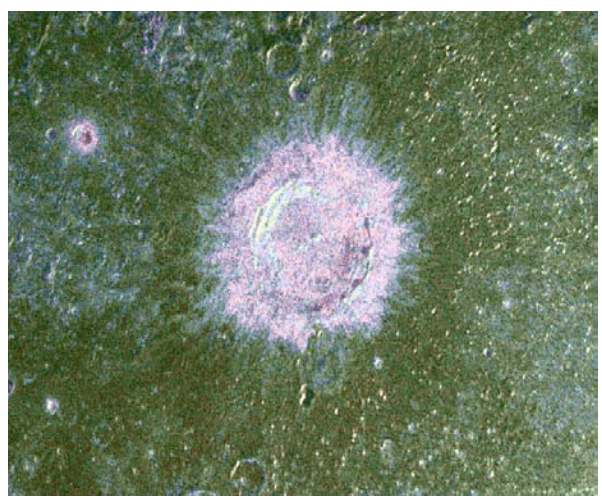

Fig. 1. 70-cm radar image of Copernicus (diameter: 93 km; crater centre: 9.7°N, -20.1°E); circular polarization ratio (color) overlain on opposite-sense image. Bright and dark haloes are apparent. The transition from bright to dark halo is gradational and might indicate a gradation in particle sizes within the ejecta.

Preliminary Results: 78 craters on the lunar nearside have been mapped thus far and all possess bright and dark haloes surrounding the crater rims. Figs. 2 and 3 show the relationship between halo and crater radii. Most of the halo margins are digitate in morphology and are not very sharp. The transitions from bright to dark haloes are also generally gradational. Furthermore, a number of craters show more than one bright halo around them, each with a slightly different brightness, representing a different concentration of blocky particles than the others.

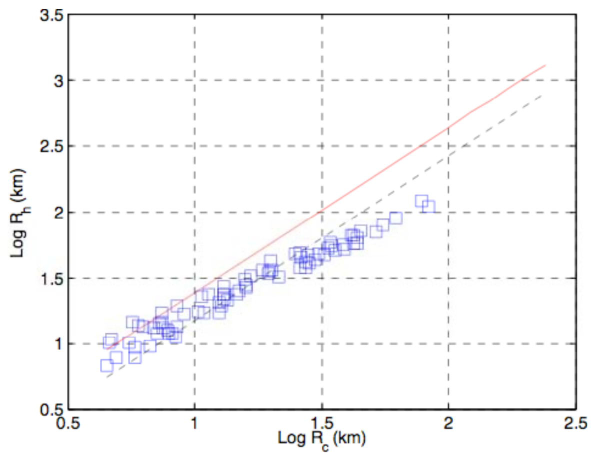

Fig. 2. Log-log plot: Bright halo radii vs. crater rim radii; red trend is a power-law curve derived in [4] using sixteen craters listed there; black-dashed trend is a curve derived using the same exponent (1.25) as the red curve, and a best-fit intercept of –0.0790.

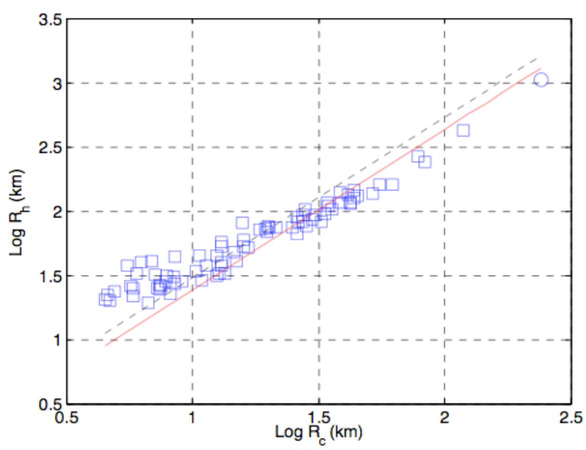

Fig. 3. Log-log plot: Dark halo radii vs. crater rim radii; red trend is a power-law curve derived in [4] using sixteen craters listed there; black-dashed trend is a curve derived using the same exponent (1.25) as the red curve, and a best-fit intercept of 0.2328.

A comparison of the observed values with the curve derived in [4] shows that for the dark haloes, a majority of the craters below a certain size fall above the red trendline. This implies that the dark haloes for these craters are larger than predicted from the previous study of craters with d ≥ 40 km. This size threshold is visible as an inflection point at approximately log R_c = 1.3 km (r_c = 20 km). This suggests that the relative volume of block-poor ejecta produced for small craters is larger than that for large craters. For the bright haloes (Fig. 3), a similar inflection point is observed, though with the opposite sense, suggesting that the proportion of blocky ejecta decreases with increasing crater size. A comparison of the two plots shows that the block-poor haloes are larger relative to their parent craters than the radar-bright haloes. This observation is potentially important to our effort to understand the processes by which these ejecta are produced and emplaced. For example, it is possible that the larger blocks are broken into finer ones on impact, producing a higher amount of block-poor ejecta.

There are several potential sources of error in the current measurements. First, we might be overestimating the sizes of large craters due to modification and enlargement of the diameters of large, fresh lunar craters by collapse of the walls into terraces [1, 6]. In addition, both the bright and dark halo margins are difficult to delineate because they are inherently gradational boundaries, which is expected to play a bigger role in the case of small craters as opposed to large craters, since a slight amount of error could be quite significant relative to the small crater size. Finally, while measuring halo sizes, an assumption was made that for each halo, the ejecta thickness was constant throughout the halo margin [4]. However, this assumption might not hold true for all cases since all bright haloes are not equally bright and all dark haloes are not equally dark.

Ongoing work involves a) continued measurements of bright and dark haloes across the entire nearside mosaic, b) integration of morphological observations with halo size observations, to serve as starting points for determining the provenance from within the crater cavity of various ejecta block size components, and ultimately, c) to begin investigating the physics of ejecta production and emplacement.

References: [1] Thompson T. W. et al. (1970) *Radio Sci., 5(2),* 253-262. [2] Thompson T. W. (1974) *Moon, 10,* 51-85. [3] Ghent R. R. et al. (2005) *JGR, 110,* E02005. [4] Ghent R. R. et al. (2008) *Geology, G24325*. [5] Thompson T. W. et al. (2006) *JGR, 111,* E06S14. [6] McGetchin T.R. et al. (1973) *Earth & Planet. Sci. Letters, 20,* 226-236.